RSC Advances

RSC Advances

www.rsc.org/advances

ROYAL SOCIETY OF CHEMISTRY

www.rsc.org/advances

Several ionic organic compounds as positive electrolyte additive for a vanadium redox flow battery

Gang Wang[1], Jinwei Chen[1], Yadong Xu[1], Bichen Yan[1], Xueqin Wang[1], Xuejing Zhu[1],

Yu Zhang[1], Xiaojiang Liu[2], Ruilin Wang[1]*[1]

(1. College of Materials Science and Engineering, Sichuan University, Chengdu

610065, China; 2. Institute of Electronics Engineering, China Academy of Engineering

Physics, Mianyang 621900, China)

Abstract

Several ionic organic compounds have been employed as additives of the V(V) electrolyte for vanadium redox flow battery (VRB) to improve its stability and electrochemical activity. Stability of the V(V) electrolyte with and without additives was investigated with ex-situ heating/cooling treatment over a wide temperature range of -5 °C to 60 °C. It was found that cationic organic compounds could significantly improve the stability of the V(V) electrolyte at a wide range of temperature. Their electrochemical behavior in the V(V) electrolyte were further studied by cyclic voltammetry (CV) and steady state polarization. The results showed that the electrochemical activity, including the reversibility of electrode reaction, the diffusivity of V(V) species, polarization resistance of V(V) species, the polarization resistance and the flexibility of charge transfer for the V(V) electrolyte with these

---
[1] * Corresponding author. Tel.: +86 2885418018; fax: +86 2885418018.

E-mail address: rlwang26@aliyun.com

additives was all improved compared with the pristine solution. The VRB employing positive electrolyte with cationic organic compounds as additive exhibited excellent charge-discharge behavior with an average energy efficiency of more than 80% at a current density of 20 mAcm^{-2}. XPS spectra illustrated that the addition of CHPTAC introduced more oxygen-containing and nitrogen-containing functional groups, which improved the electrochemical performance and cycling stability of VRB.

Keywords: *Vanadium redox flow battery; V(V) electrolyte; ionic organic additives; Stability; Electrochemical behavior*

1 Introduction

More and more researchers have been paying attention to large-scale electrical energy storage since the energy crises of the 1970s. All vanadium redox flow battery (VRB in short), as one of the most promising redox flow battery technologies for large-scale electrical energy storage, was pioneered by M. Skyllas-Kazacos group at UNSW in Australia[1]. The VRB overcomes the inherent problem of cross contamination due to the diffusion of different redox ions across the membrane, which occurs in all other redox flow batteries. By employing the V(V)/V(IV) and V(III)/V(II) redox couples in H_2SO_4 as the positive and negative half-cell electrolytes respectively, the capacity and power output of VRB are dependent on the volume and concentration of the electrolyte[2-6]. However, the low energy density of the vanadium sulphate electrolyte (20−35 Wh/kg)[7] due to the low solubility and stability of the active vanadium species at elevated temperature, especially for V(V) species in the electrolyte of VRB limits its use to stationary systems.

$$2[VO_2(H_2O)_3]^+ - 2H^+ \longrightarrow 2VO(OH)_3 + 2H_2O \quad (1)$$

$$2VO(OH)_3 \longrightarrow V_2O_5 + 3H_2O \quad\quad\quad (2)$$
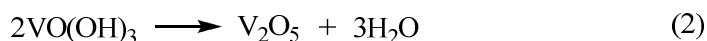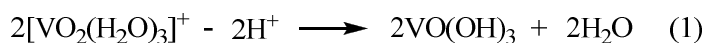
V(V) species exist in a relatively stable structure of $[VO_2(H_2O)_3]^+$ in H_2SO_4 at low

temperatures. When the temperature increases, the structure will deprotonate and

produce a neutral structure of $VO(OH)_3$ (1), which will ultimately lead to the

formation of the crystallization of V_2O_5 (2)[8]. The rate and extent of precipitation in

the V(V) solution were found to be mainly controlled by the solution temperature, the

vanadium concentration, the sulfuric acid concentration, and the state of charge (SOC)

of the electrolytes[9, 10].

In the past years, great efforts have been made to increase the stability of V(V)

species in H_2SO_4, aimed at developing high concentration, stable vanadium

electrolyte for VRB system[11-29]. It was found that the stability of V(V) electrolyte

can be improved by increasing the concentration of H_2SO_4, decreasing the

concentration of V(V) species to below 1.8 M and adjusting the temperature at 10 °C

to 40 °C. But the high concentration of H_2SO_4 favors the precipitation of V(II), V(III)

and V(IV) species[30], the concentration below 1.8 M would greatly decrease the

energy density of VRB[2], and the temperature controlled over 10 °C to 40 °C would

limit the practical applications of VRB[31]. Adding stabilizing agents into electrolyte

is thought to be one of the most economic and effective methods for preventing and

delaying the precipitate formation[32]. Surfactants, such as Coulter dispersants[21]

and cetyltriethylammnonium bromide(CTAB)[22], carboxylic acids compounds

[12,17,26,29], alcohols compounds containing –OH, –SH, or –NH$_2$ groups with ring

or chain structures at tertiary carbon atoms[12-16,18-20,23-25,28] were reported as potential stabilizing agents for V(V) electrolyte, which could encapsulate the hydrated form of V(V) species and inhibit the precipitation formation[12].

Based on these reports, several new ionic organic additives were added into the V(V) electrolyte and corresponding effects on thermal stability at different temperature, electrochemical kinetic behavior were studied and compared with the pristine solution. Moreover, the additives with good performance in V(V) anolyte solutions were tested by charge-discharge technique.

2 Experimental

2.1 Preparation of V(V)

The V(V) electrolyte solutions were prepared through two processes as follows: high concentration V(IV) electrolyte solutions were prepared by electrolytic dissolution of V_2O_5 (analytical reagent, AR) in 3.0 M H_2SO_4 supporting electrolyte; then high concentration (V) electrolyte solutions were obtained by charging the prepared V(IV) electrolyte solutions. Both the two processes were conducted in a two-compartment electrolysis cell[18,19,21,33] with a separator of low price ion exchange membrane. And 1.8-2.8 M V(V) / 5.0 M H_2SO_4 electrolyte solutions were gained by adjusting the prepared high concentration V(V) electrolyte solutions with 98 wt% H_2SO_4 and deionized water. The valence and concentration of the vanadium ions in the electrolyte were measured by 916 Ti-Touch (Metrohm) potentiometric titrator.

2.2 Stability experiment of V(V)

The tests were carried out in sealed glass tubes over a temperature range of -5 °C to 60 °C in a temperature-controlled bath for 30 days. To investigate the additive effect on high concentration V(V) anolyte (2.8 M V(V) / 5.0 M H_2SO_4), a certain amount of additives were added into the glass tubes with electrolyte solutions, and then argon gas was piped into the glass tubes for several minutes to remove oxygen before starting the stability tests. All the stability tests were carried out statically (i.e., without any agitation). During the tests, each sample was visually monitored and recorded more than twice a day for slight precipitation of V_2O_5. At the end of the 30-day test period, the solutions were filtered and the 'equilibrium' vanadium species concentration determined by potentiometric titrator analysis again.

2.3 Electrochemical measurements

Cyclic voltammetry (CV) tests and steady polarization study of 2.8 M V(V) / 5.0 M H_2SO_4 electrolyte solutions with and without additives were performed using the CHI 600B electrochemical workstation (Shanghai Chenhua Instrument, China) in a temperature-controlled bath at -5 °C, 25 °C and 45 °C. The curves of current versus potential were recorded in a 3-electrode electrochemical cell using graphite electrode as the working electrode (surface area 3.14 mm^2), saturated mercurous sulfate electrode as the reference electrode, and platinum electrode as the counter electrode. Prior to test, the working electrode was manually polished with 0.3 μm and 0.5 μm

α-Al$_2$O$_3$ power and then washed by ultrasonic cleaning in ethanol and distilled water

for 5 min, respectively.

2.4 Cell tests

The single VRB cell was composed of two pieces of graphite felt (the thickness

was 10 mm, Hunan Jiuhua Carbon Hi-Tech Co., Ltd.), two current collectors (Zibo

Jinpeng Carbon Co., Ltd.) and a PE-PSSA composite ion exchange membrane

(Zhejiang Qianqiu Group Co., Ltd., China) (Fig. 1). The active area of the electrode

was about 30 cm^2. 70 mL of 1.8 M V(IV)/ 3.0 M H$_2$SO$_4$ solutions with 0.5 wt%

different additives and 70 mL of 1.8 M V(III)/ 3.0 M H$_2$SO$_4$ solutions (obtained by

further electrolyzing the prepared V(IV) solutions) were used as the initial anolyte and

catholyte respectively, and cyclically pumped into the corresponding half-cell by a

peristaltic pump. The catholyte was bubbled with N$_2$ for 5 min to clear O$_2$ and then

sealed to prevent oxidation. The flow rate of the peristaltic pump was fixed at 50

mL/min. The galvano-static charge and discharge of the test cell were carried out by

CT2001A-5V/2A (Wuhan Land Co., China) between 0.8 V and 1.6 V at a current

density of 20 mA cm^{-2}.

(Fig. 1 about here)

2.5 X-ray photoelectron spectroscopy (XPS)

X-ray photoelectron spectroscopy (XPS) of graphite felts were conducted on

6

K-Alpha 1063 (Thermo Fisher Scientific, UK) with Al Kα X-ray source generated at

12 kV and 6 mA in an ultra-high vacuum of about 10^{-9} mBar. The graphite felts

obtained from the cycling tests were washed by deionized water and ultrasonic

cleaning in deionized water to remove the electrolyte and impurities, and then dried in

an oven at 120 °C for 2 h.

3 Results and discussion

3.1 Effect of additives on stability of V(V)

Most additives could affect the stability of vanadium electrolyte solutions to

some extent. Several ionic organic additives (0.5 wt%) (Table 1) were selected to

investigate the additive effect on thermal stability of 2.8 M V(V)/ 5.0 M H_2SO_4

electrolyte over a wide temperature range of -5 °C to 60 °C.

As shown in Table 2, the stability of V(V) solution without additives decreased

greatly when the temperature increased from -5 °C to 60 °C due to the endothermic

nature of the precipitation reaction of the V(V) species[9]:

$$2VO_2^+ + H_2O \longrightarrow V_2O_5 + 2H^+ \quad \Delta H > 0 \quad (3)$$
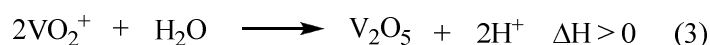
The change of the stability with temperature could be related to the formation of

different V(V) species at different temperatures[17]. The stability of V(V) solution

could be improve by adding additives at the same temperature. Compared with the

results in the pristine solution, most of the studied additives could improve the

stability of V(V) solution. For example, the pristine sample suffered from

precipitation within only 18 h at 45 °C, while the V(V) solution with ionic methylene

blue (MB) kept stable without any precipitation within 30 days at 45 °C, indicating

that MB could significantly improve the stability of the V(V) solution. Other ionic

organic additives, such as 3-chloro-2hydroxypropyl trimethyl ammonium chloride

(CHPTAC), Tetrabutyl ammonium bromide (TBAB), potassiumacidphthalate (PAP),

cationic polyacrylamide (CPAM) and polyacrylamide (APAM) could also improve the

stability of the V(V) solution from -5 °C to 60 °C.

At the same time, the concentration of V(V) solution with and without additives

was monitored after 30 days at -5 °C, 10 °C and 30 °C, respectively. As listed in Table

2, the concentration of all V(V) solution was observed to decrease with increasing

temperature, which was consistent with the stability tests above. The concentration of

V(V) solution could be remained at a certain degree through adding additives. It was

found that the concentration of V(V) solution with most ionic organic additives, such

as CHPTAC, TBAB and PAP, remained more than 2.0 M after 30 days, which would

be helpful to increase energy capacity over the current sulfate system of VRB[3].

However, MB was oxidized by the V(V) species due to the reduction of the lone pair

electrons on the nitrogen atoms [12-16], maintaining a lower concentration of 1.9 M at

30 °C after 30 days.

The results obtained through adding ionic organic additives at a certain

temperature may be interpreted that the hydrated form of V(V) species were

encapsulated by amphiphilic micellar structures[13,23] of the additives, which made

the V(V) species more diffuse, finally delayed and inhibited the formation of

precipitation. In addition, synergy of coulombic repulsion and steric hindrance

between these additives and the hydrated form of V(V) species could also improve the stability of the V(V) solution[8,21,23,24].

However, the results showed that CPAM and APAM were more likely to precipitate compared with the other organic additives. Both CPAM and APAM were polymers and had large volume charged groups, the charges of which were more scattered than micromolecule. So this might lead to weak interaction between the scattered charges and V(V) species, which could not prevent V(V) species aggregation effectively.

The additives CHPTAC, MB, TBAB and PAP can be used as promising stabilizing agents for V(V) electrolyte through further optimize the quantity of addition and the range of temperature.

(Table 1 about here)

(Table 2 about here)

3.2 Cyclic voltammetry

(Fig. 2 about here)

As seen in Fig. 2, the CV curves of the test solutions with and without ionic organic additives had identical peak positions and patterns, and were similar to each other in peak shape, which exhibited evidently only one couple of redox peaks.

However, the reversibility of V(V)/V(IV) redox couple with additives was changed in three aspects. Firstly, the separation between the oxidation and reduction peak potential (ΔV_p), and the ratios of oxidation peak current to reduction peak current (I_{pO}/I_{pR}) of the solutions with additives were both changed compared with that of the pristine solution. Most of the additives could decrease the ΔV_p and make I_{pO}/I_{pR} close to one, which improved the reversibility of V(V)/V(IV) redox couple at a certain extent. Secondly, the increasing of the oxidation and reduction peak currents were observed when most of the additives were added into the test solution, which indicated the improvement of electrode reaction kinetics[20,36]. Finally, further study on the reversibility of V(V)/V(IV) redox couple with additives was carried out through monitoring the ΔV_p, I_{pO}/I_{pR} and peak currents at a lower (-5 °C) and higher temperature (45 °C), respectively. The CV tests of the ΔV_p, I_{pO}/I_{pR} and peak currents at -5 °C and 45 °C showed the similar results compared with 25 °C. As shown in Table 3, compared with the results in the pristine test, most of the studied additives could improve the electrode reaction kinetics and the reversibility of V(V)/V(IV) redox couple at different temperature. Taking the test solutions with 0.5 wt% CHPTAC and MB for example, the ΔV_p were reduced, the I_{pO}/I_{pR} were closer to one and the peak currents were increased at a certain temperature comparing to the pristine test solution. Their peak currents were also found to increase with the increasing of temperature due to the improvement of electrode reaction kinetics (Fig. 3). In addition, the cyclic stability of V(V) solutions with different additives was tested by continuous CV scans for 50 cycles at a scan of 50 mV/s at a graphite

electrode at -5 °C and 45 °C. It was found that almost no variation was observed on

the peak shape and the peak potential separation, suggesting that the V(V) electrolyte

with 0.5 wt% CHPTAC (Fig. 4(a)) and MB (Fig. 4(b)) at -5 °C and 45 °C both had

good cycling stability. The results indicated that the reversibility and cyclic stability of

the test solutions with CHPTAC and MB was improved. The similar results were also

found in the test solutions with TBAB and PAP. As ionic organic additives or

analogous surfactants, CHPTAC, MB, TBAB and PAP could provide reaction sites for

V(V)/V(IV) redox couple and quicken the process of charge transfer[22], and finally

improve the electrochemical reversibility and cyclic stability of V(V)/V(IV) redox

couple. Moreover, CHPTAC contained –OH groups that could complex with

V(V)/V(IV) ions in the solution and provide available –OH groups for the

ion-exchange between V(V)/V(IV) ions and –OH groups on electrode surface, which

would lead to high oxidation and reduction peak currents and the improvement of the

electrochemical reversibility and cyclic stability of V(V)/V(IV) redox

couple[18-20,25]. However, the large volume ionic groups of CPCM and APCM

hindered the process of charge transfer and ion-exchange on electrode surface, and

lead to low electrochemical activity. The results was consistent with the thermal

stability tests above.

(Table 3 about here)

(Fig. 3 about here)

(Fig. 4 about here)

In order to further investigate the effect of additives on the kinetics of electrode reaction, a series of CV curves for test solutions containing with 0.5 wt% CHPTAC and MB on the graphite electrode at various scan rates were shown in Fig. 5 (a) and (c). It presented the typical characteristics of a quasi-reversible one-electron process for the oxidation and reduction peak potentials changed gradually with the scanning rates[19,30,31]. A plot of the oxidation peak currents as a linear function of the square root of scan rates with additives of 0.5 wt% CHPTAC and MB (Fig. 5 (b) and (d)) further verified the quasi-reversible process for V(V)/V(IV) redox reaction.

(Fig. 5 about here)

Theoretically, the value of the diffusion coefficient for a quasi-reversible reaction (D) is between that for a reversible (D_1) one and an irreversible (D_2) one[34]. For a reversible and irreversible one-step and one-electron reaction, the peak current i_p is given in Eqs. (4) and (5), respectively[35]:

$$i_p = 0.4463 \, (F^3/RT)^{1/2} \, ACD_1^{\,1/2} \upsilon^{1/2} \quad \text{(reversible reaction)} \tag{4}$$

$$i_p = 0.4958 \, (F^3/RT)^{1/2} \, \alpha^{1/2} \, ACD_2^{\,1/2} \upsilon^{1/2} \quad \text{(irreversible reaction)} \tag{5}$$

where F is the Faraday constant, R is the universal gas constant, T is the Kelvin temperature, A is the surface area of working electrode, C is the bulk concentration of

primary reactant, D_1 and D_2 refer to the diffusion coefficient for a reversible reaction and a irreversible reaction, respectively. υ is the scanning rate. α refers to the transfer coefficient for a reversible reaction.

For a one-step and one-electron reaction at different temperature, the similar Eqs. of the peak current i_p can be deduced base on Eqs. (4) and (5). For example, when $T = 25\ °C = 298.15$ K, Eqs. (4) and (5) can be transformed as follows:

$$i_p = 2.69 \times 10^5\, ACD_1^{1/2} \upsilon^{1/2} \tag{6}$$

$$i_p = 2.99 \times 10^5\, \alpha^{1/2} ACD_2^{1/2} \upsilon^{1/2} \tag{7}$$

Based on the known experimental conditions, Eqs. (6) and (7) can be further transformed as follows:

$$i_p/A = 538\, D_1^{1/2} \upsilon^{1/2} = k\upsilon^{1/2} \tag{8}$$

$$i_p/A = 598\, D_2^{1/2} \upsilon^{1/2} = k\upsilon^{1/2} \tag{9}$$

It is found that k refers to the slope of the line in point of the linear Eqs. (8) and (9), where the variables are the current density i_p/A and the square root of scan rate $\upsilon^{1/2}$. k can be determined by the linear regression. D_1 and D_2 can be calculated by using the following Eqs. (10) and (11):

$$D_1 = 3.45 \times 10^{-6}\, k^2 \tag{10}$$

$$D_2 = 2.80 \times 10^{-6}\, k^2 \tag{11}$$

According to Eqs. (10) and (11), it is observed that the diffusion coefficient D increases with the slope k increasing, which refers to the enhanced diffusivity of primary reactant. For a reversible redox couple, such as V(V)/V(IV), the similar process of derivation and calculation above about the diffusion coefficient D at

different temperature can be reused.

Herein, the slope k was fitted and obtained according to the oxidation peak current i_p. The diffusion coefficient D_1 and D_2 of (V) species with different ionic organic additives at different temperature were listed in Table 4. It was observed that the diffusion coefficient D (D_1 to D_2) increased with the temperature increasing, affected the electrode reaction diffusion kinetics of (V) species and intensified the processes of mass transfer and charge transfer for V(V)/V(IV) redox couple. Moreover, the diffusion coefficients of the test solutions with most of additives increased at a certain temperature comparing to the pristine test solution, indicating that ionic organic additives could improve the diffusion of V(V) species on the electrode. As a result, the corresponding reaction activity was improved. For example, the diffusion coefficient of V(V) species with additives of 0.5 wt% CHPTAC and MB was increased from $1.27–1.57×10^{-6}$ cm^2 s^{-1} (pristine) to $1.73–2.13×10^{-6}$ cm^2 s^{-1} and $1.52–1.88×10^{-6}$ cm^2 s^{-1} at 25 °C, respectively. The analogous results were also found of V(V) species with additives of 0.5 wt% TBAB and PAP, which was consistent with the stability and CV tests.

(Table 4 about here)

3.3 Steady state polarization

(Fig. 6 about here)

The steady polarization curves for V(V) solution with different acid additives were employed to determine the polarization resistance, exchange current density, and electrochemical reaction rate constant. In relatively low overvoltage area, current density and overvoltage should yield an approximate straight line. Polarization resistance could be calculated by the slope of the line and other parameters such as exchange current density and electrochemical reaction rate constant could be calculated as follows[19]:

$$R_p = \frac{\eta}{i_0}, \quad i_0 = \frac{RT}{nFR_p}, \quad k_0 = \frac{i_0}{nFC_0} \tag{12}$$

where i_0 is the exchange current density, R is the universal gas constant, T is the Kelvin temperature, n is the number of electrons transferred in the reaction, F is the Faraday constant, R_p is the polarization resistance, k_0 is rate constant, and C_0 is the solution concentration.

(Table 5 about here)

The steady polarization curves for 2.8 M V(V) / 5.0 M H_2SO_4 with different acid additives on the graphite electrode were shown in Fig.6 and the corresponding parameters containing polarization resistance, exchange current density and electrochemical reaction rate constant obtained from Eq. (12) were summarized in Table 5. It was found that the polarization resistance decreased, while the exchange current density and electrochemical reaction rate constant increased with the

temperature increasing, which accelerated the kinetic process of V(V) species. Moreover, comparing to the pristine solution, the polarization resistance decreased and the exchange current density and electrochemical reaction rate constant increased for the V(V) solution with most of ionic organic additives. For example, the polarization resistance of V(V) solution with additives of 0.5 wt% CHPTAC and MB decreased from 4.24 Ωcm^2 (pristine) to 3.77 Ωcm^2 and 3.82 Ωcm^2 at 25 °C, respectively. Meantime, the exchange current density of V(V) solution with additives of 0.5 wt% CHPTAC and MB increased from 6.06 $mAcm^{-2}$ (pristine) to 6.81 $mAcm^{-2}$ and 6.72 $mAcm^{-2}$, and electrochemical reaction rate constant increased from $2.24\times10^{-5}cm\ s^{-1}$ (pristine) to $2.52\ \times10^{-5}cm\ s^{-1}$ and $2.49\ \times10^{-5}cm\ s^{-1}$ at 25 °C, respectively. The similar results were also found of V(V) species with additives of 0.5 wt% TBAB and PAP, which was consistent with the stability and CV tests. The V(V) solution with these additives had a faster kinetic process on the graphite electrode probably due to the improved diffusion and oxidation ability of the V(V) species[19].

3.4 Electrochemical impedance spectroscopy

(Fig.7 about here)

In order to further analyze the electrode reaction diffusion kinetics of (V) species and the processes of mass transfer and charge transfer for V(V)/V(IV) redox couple, electrochemical impedance spectra were used to record Nyquist plots of the

electrolyte with and without ionic organic additives at room temperature. As shown in

Fig.7, each plot consisted of a semicircle in the high frequency region and a sloped

line in the low frequency region, indicating that the redox reaction of V(V)/V(IV)

couple was simultaneously controlled by the charge transfer process at high frequency

and the diffusion process at low frequency[18,19]. Consequently, the Nyquist plots

could be fitted with the equivalent circuit of Fig.7. In the equivalent circuit, R_1 stands

for the resistance composed of solution resistance, electrode resistance and the contact

resistance. R_2 and W represent the charge transfer resistance and Warburg diffusion

impedance in the electrochemical process, respectively. CPE is the constant phase

element represents the electric double-layer capacitance of the electrode/solution

interface[18,19].

(Table 6 about here)

The simulation results obtained by Zsimpwin software from fitting the

impedance plots with the equivalent circuit model in Fig.7 were shown in Table 6. It

was observed that there were significant differences in R_1 and R_2 for each sample and

the electrolytes with ionic organic additives exhibited a lower electrolyte resistance

and charge transfer resistance than the pristine one, which indicated that the transfer

of V(V) species and electron were more feasible after adding 0.5 wt% CHPTAC, MB,

TBAB and PAP[18,19]. For example, the R_1 and R_2 of V(V) species with additive of

0.5 wt% CHPTAC was decreased from 0.2748 Ωcm^2 (pristine) to 0.2372 Ωcm^2 and

0.3905 Ωcm^2 (pristine) to 0.1243 Ωcm^2, respectively. Moreover, the parameter $Y_{0,1}$

for the electrolyte was increased after adding these additives, indicating enhancements

of the electric double-layer capacitance of the electrode/electrolyte interface[18-20].

Meantime, the admittance of Warburg diffusion impedance $Y_{0,2}$ was also increased

and exhibited a lower diffusion impedance after adding these additives. The results

above further verified that the electrochemical activity of V(V) electrolytes could be

improved through adding 0.5 wt% CHPTAC, MB, TBAB and PAP.

3.5 Charge and discharge tests

(Fig. 8 about here)

The charge-discharge tests were performed on a single VRB cell mentioned

above. As shown in Fig.8(a), the charge-discharge curves of positive electrolytes with

most additives presented a lower charging voltage and higher discharging voltage than

the pristine one at room temperature, which indicated additives could improve the

performance of VRB. For example, VRB with 0.5 wt% CHPTAC showed a higher

coulombic, voltage and energy efficiency compared with the pristine one (Fig.8(b)).

The coulombic efficiency increased from 92% (pristine) to 94% (with 0.5 wt%

CHPTAC), voltage efficiency increased from 88.2% (pristine) to 91.6% (with 0.5

wt% CHPTAC) and energy efficiency increased from 81.1% (pristine) to 86.1% (with

0.5 wt% CHPTAC). The similar results could also be observed for other additives,

such as MB, TBAB and PAP, which was consistent with the thermal stability, CV and polarization tests. It was likely due to that the ions of ionic organic additives blocked the aggregation of the V(V) ions and reduced V_2O_5 precipitation and thus increased the efficiency of VRB.

(Fig. 9 about here)

In order to further investigate the effect of ionic additives on cycling stability, VRB with and without 0.5 wt% CHPTAC in the positive electrolyte were monitored as an example. Fig. 9 showed the coulombic, voltage and energy efficiency of VRB as a function of cycling number (20 cycles) and compared the VRB performance with and without 0.5 wt% CHPTAC. As the cycles proceeded, VRB showed slight fluctuations in the coulombic, voltage and energy efficiency. It would take some time to reach dynamic equilibrium for infiltration and interaction between the electrolyte and electrode[21]. With the increasing of circle numbers, the performance of VRB with 0.5 wt% CHPTAC kept stable and remained above 92 % of coulombic efficiency, 86 % of voltage efficiency and 81% of energy efficiency at the current density of 20 mA cm^{-2}, respectively, which was better than the pristine one. The result indicated that ionic organic additive could improve the cycling stability of VRB.

3.6 X-ray photoelectron spectroscopy

(Fig. 10 about here)

(Table 7 about here)

To investigate the effect of functional groups in ionic additives on the surface of graphite felts after cycling tests, the XPS spectra of the graphite felt in the positive electrolyte with and without 0.5 wt% CHPTAC after cycling tests were measured in the binding energy charge of 1-1100 eV as an example. As shown in Fig. 10, the peaks for carbon (C), oxygen (O) and nitrogen (N) were centered on 284, 532 and 401 eV, which demonstrated the existence of -OH and quaternary N functional groups of CHPTAC. The intensity of O 1s and N 1s peaks for the graphite felt in the positive electrolyte with 0.5 wt% CHPTAC were stronger than that of pristine one. The relative contents of the elements on the surface of graphite felts were specified in Table 7. Comparing with the pristine one, the content of O and N for the graphite felt in the positive electrolyte with 0.5 wt% CHPTAC increases from 19.57 % to 33.77 % and 1.51 % to 4.63 %, respectively. The result indicated that the CHPTAC in the positive electrolyte significantly increased the amount of -OH and quaternary N functional groups on the surface of the electrode, which could provide more active sites for the V(V)/V(IV) redox reaction and enhance hydrophilic property of the electrode, and further accelerate the electrochemical reaction[18, 25, 28]. Moreover, the CHPTAC in the positive electrolyte could also supplement the loss of oxygen-containing and nitrogen-containing functional groups on the graphite felt electrode during cycling tests, and thus improved the cycling stability of VRB[28].

4 Conclusion

The stability and electrochemical behavior of the V(V) electrolyte with and without several additives were studied and compared. The results showed that V(V) electrolyte with ionic compound CHPTAC, MB, TBAB and PAP remained stable over a wide temperature range of -5 °C to 45 °C. The electrochemical activity, including the reversibility of electrode reaction, the diffusivity and polarization resistance of V(V) species and the flexibility of charge transfer of V(V)/V(IV) redox couple for the V(V) electrolyte with these additives was found to be improved compared with the pristine solution. The charge-discharge tests indicated that VRB with 0.5 wt% CHPTAC, MB, TBAB and PAP had higher coulombic, voltage and energy efficiency compared with the pristine solution. In addition, CHPTAC could significantly improve the cycling stability of VRB most likely due to its ionic quaternary N and -OH functional groups. Through further optimize molecular structures, quantity of addition and the range of temperature, these additives can be used as promising stabilizing agents for V(V) electrolyte in practical application.

University (XTCX2011001).

Reference

[1] M. Skyllas-Kazacos, R. G. Robins, AU Patent 0,575,247 (1986)

[2] M. Skyllas-Kazacos, M. H. Chakrabarti, S. A. Hajimolana, F. S. Mjalli, M. Saleem, J. Electrochem. Soc., 158 (2011) R55－R79.

[3] Z. G. Yang, J. L. Zhang, M. C. W. Kintner-Meyer, X. C. Lu, D. W. Choi, J .P. Lemmon, J. Liu, Chem. Rev.,111 (2011) 3577－3613.

[4] P. K. Leung, X. Li, C. Ponce de Léon, L. Berlouis, C. T. J. Low, F.C. Walsh, RSC Adv., 2 (2012),10125－10156.

[5] G. Kear, A. A. Shah, F. C. Walsh, Int. J. Energy Res., 36 (2011) 1105－1120.

[6] M. J. Watt-Smith, H. Al-Fetlawi, P. Ridley, R. G. A. Wills, A. A. Shah, F. C. Walsh, J. Chem. Technol. Biot., 88 (2013) 126－138.

[7] M. Skyllas-Kazacos, G. Kazacos, G. Poon, and H. Verseema, Int. J. Energy Res., 34 (2010) 182－189.

[8] M. Vijayakumar, L. Y. Li, G. Graff, J. Liu, H. M. Zhang, Z. G. Yang, J. Z. Hu, J. Power Sources 196 (2011) 3669－3672.

[9] F. Rahman, M. Skyllas-Kazacos, J. Power Sources 189 (2009) 1212－1219.

[10] M. Kazacos, M. Cheng, M. Skyllas-Kazacos, J. Appl. Electrochem., 20 (1990) 463－467.

[11] M. Skyllas-kazacos, AU Patent 8,800,472 (1989).

[12] M. Kazacos, M.Skyllas-Kazacos, US Patent 7,078,123 (2006).

[13] M. Skyllas-Kazacos, US Patent 6,143,443 (2000).

[14] M. Skyllas-Kazacos, M. Kazacos, A. Mohammed, WO Patent 9,512,219 (1994).

[15] M. Kazacos, M. Skyllas-Kazacos, US Patent 6,468,688 (2002).

[16] M. Skyllas-Kazacos, M. Kazacos, US Patent 6,562,514 (2003).

[17] J. L. Zhang, L. Y. Li, Z. M. Nie, B. W .Chen, M. Vijayakumar, S. Kim, W. Wang, B. Schwenzer, J. Liu, Z. G .Yang, J. Appl. Electrochem., 41 (2011) 1215－1221.

[18] S. Li, K. L. Huang, S. Q. Liu, D. Fang, X. W. Wu, D. Lu, T. Wu, Electrochim. Acta 56 (2011) 5483－5487.

[19] X. J. Wu, S. Q. Liu, N. F. Wang, S. Peng, Z. X. He, Electrochim. Acta 78 (2012) 475－482.

[20] Z. J. Jia , B. G. Wang , S. Q. Song , X .Chen, J. Electrochem. Soc., 159 (2012) A843－A847.

[21] F. Chang, C. W. Hu, X. J. Liu, L. Liu , J. W. Zhang, Electrochim. Acta 60 (2012) 334－338.

[22] X. W. Wu, X. Q. Liu, K. L. Huang, J. Inorg. Mater., 25 (2010) 641－645.

[23] S. Peng , N. F. Wang, C. Gao, Y, Lei, X. X. Liang, S. Q .Liu , Y. N. Liu, Int. J. Electrochem. Sci., 7 (2012) 4314－4321.

[24] S. Peng , N. F. Wang, C. Gao, Y, Lei, X. X. Liang, S. Q .Liu , Y. N. Liu, Int. J. Electrochem. Sci., 7 (2012) 4388－4396.

[25] G. Wang, J. W. Chen, X. Q Wang, J. Tian, H. Kang, X. J. Zhu, Y.Zhang, X. J. Liu, R. L. Wang, J. Electroanal. Chem. 709 (2013) 31－38.

[26] G. Wang, J. W. Chen, X. Q Wang, J. Tian, H. Kang, X. J. Zhu, Y.Zhang, X. J. Liu,

R. L. Wang, J. Energy Chem. 23 (2014) 73－81.

[27] S. K. Park, J. Shima, J. H. Yang, C. S. Jin, B. S. Lee, Y. S. Lee, K. H. Shin, J. D. Jeon, Electrochim. Acta 121 (2014) 321－327.

[28] J. L. Liu, S. Q. Liu, Z. X. He, H. G. Han, Y. Chen, Electrochim. Acta 130 (2014) 314－321.

[29] H. G. Han, Z. X. He, J. L. Liu, Y. Chen, S. Q. Liu, Ionics (2014) 1-8.

[30] F. Rahman, M. Skyllas-Kazacos, J. Power Sources 72 (1998) 105－110.

[31] M. Skyllas-Kazacos , C. Menictas, J. Electrochem. Soc., 143 (1996) L86－L88.

[32] M. Skyllas-Kazacos, M. Rychick, R. Robins, US Patent 4,786,567 (1988).

[33] G. Oriji, Y. Katayama, T. Miura, Electrochim. Acta 49 (2004) 3091－3095.

[34] F. Huang, Q. Zhao, C. H. Luo, G. X. Wang, K. P. Yan, D. M. Luo, Chinese Science Bulletin, 57(32) 2012, 4237－4243.

[35] A. J. Bard, L. R. Faulkner. Electrochemical Methods－Fundamentals and Applications. New York: Wiley, 2001. Part 6, 231－236.
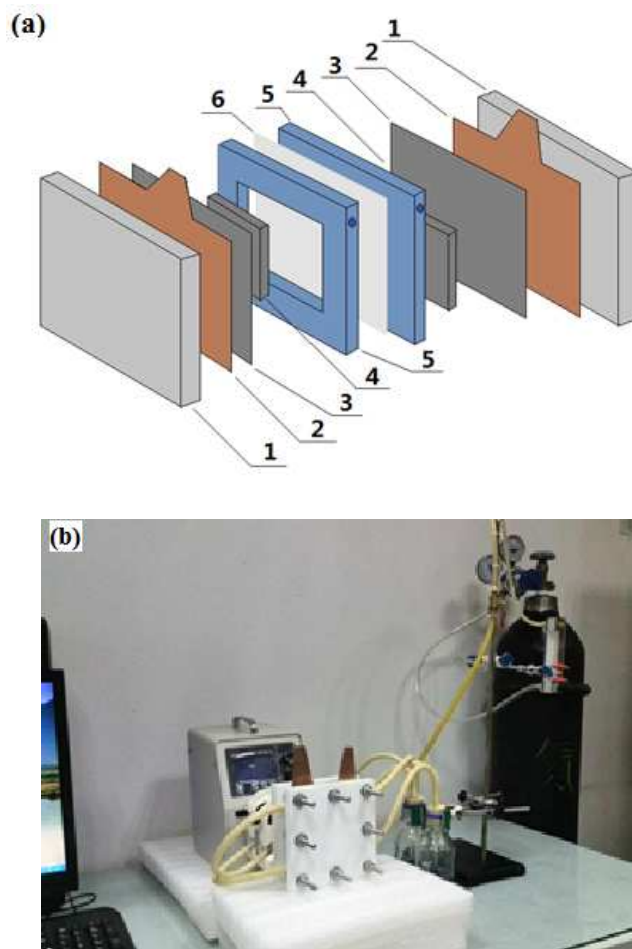
Figure Captions

Fig. 1 (a) A scheme of the cell configuration and (b) picture of the single VRB cell.
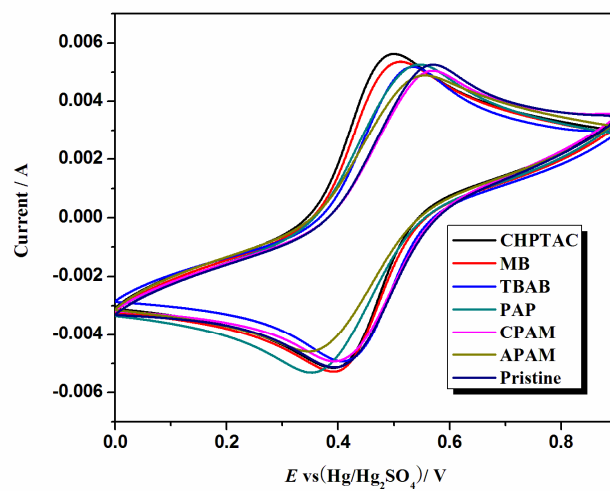
25

Fig. 2 CV curves of the electrolyte (2.8 M V(V) / 5.0 M H_2SO_4) with 0.5 wt% ionic

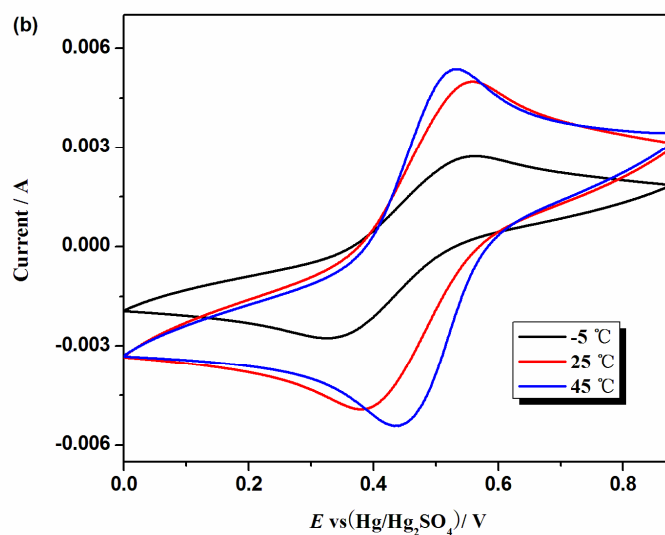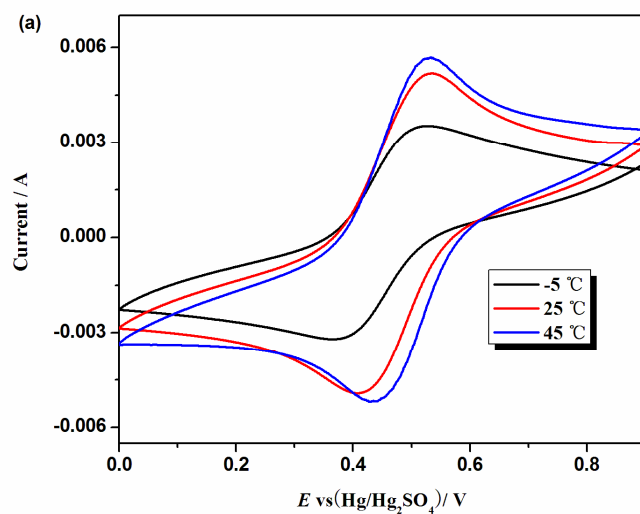organic additives on graphite electrode at room temperature at a scan rate of 50 mVs^{-1}.

Fig. 3 CV curves of the electrolyte (2.8 M V(V) / 5.0 M H_2SO_4) with (a) 0.5 wt%

CHPTAC and (b) 0.5 wt% MB on graphite electrode at different temperature at a scan
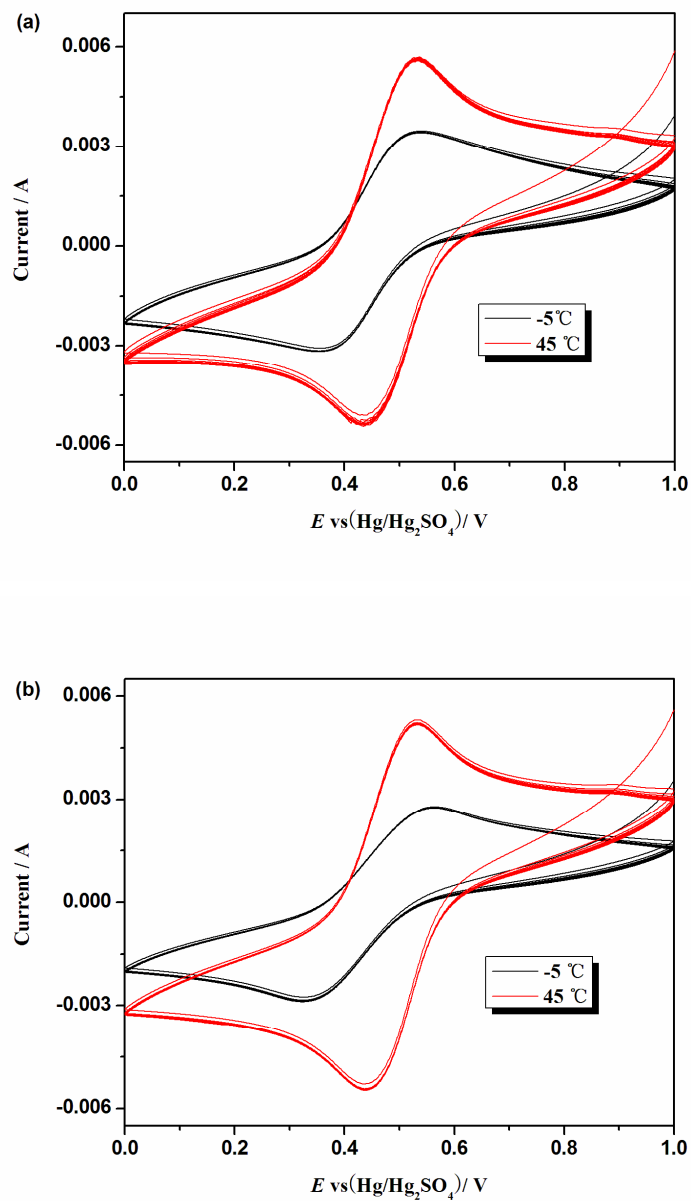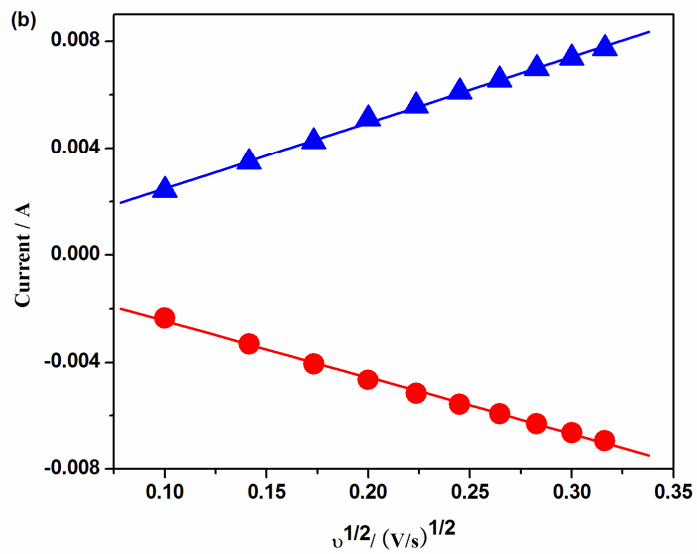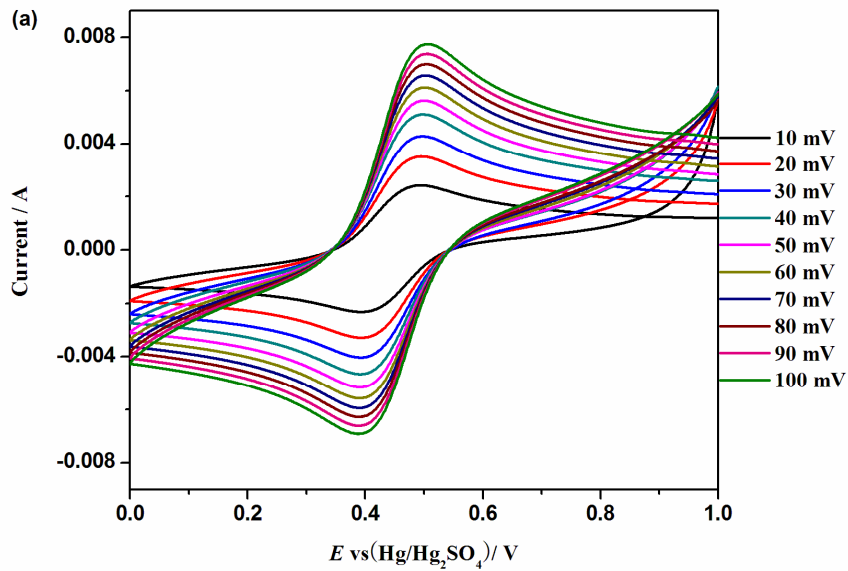
rates of 50 mV s^{-1}.

Fig. 4 CV curves (50 cycles) of the electrolyte (2.8 M V(V) / 5.0 M H$_2$SO$_4$) with (a)

0.5 wt% CHPTAC and (b) 0.5 wt% MB on graphite electrode at -5 °C and 45 °C at a
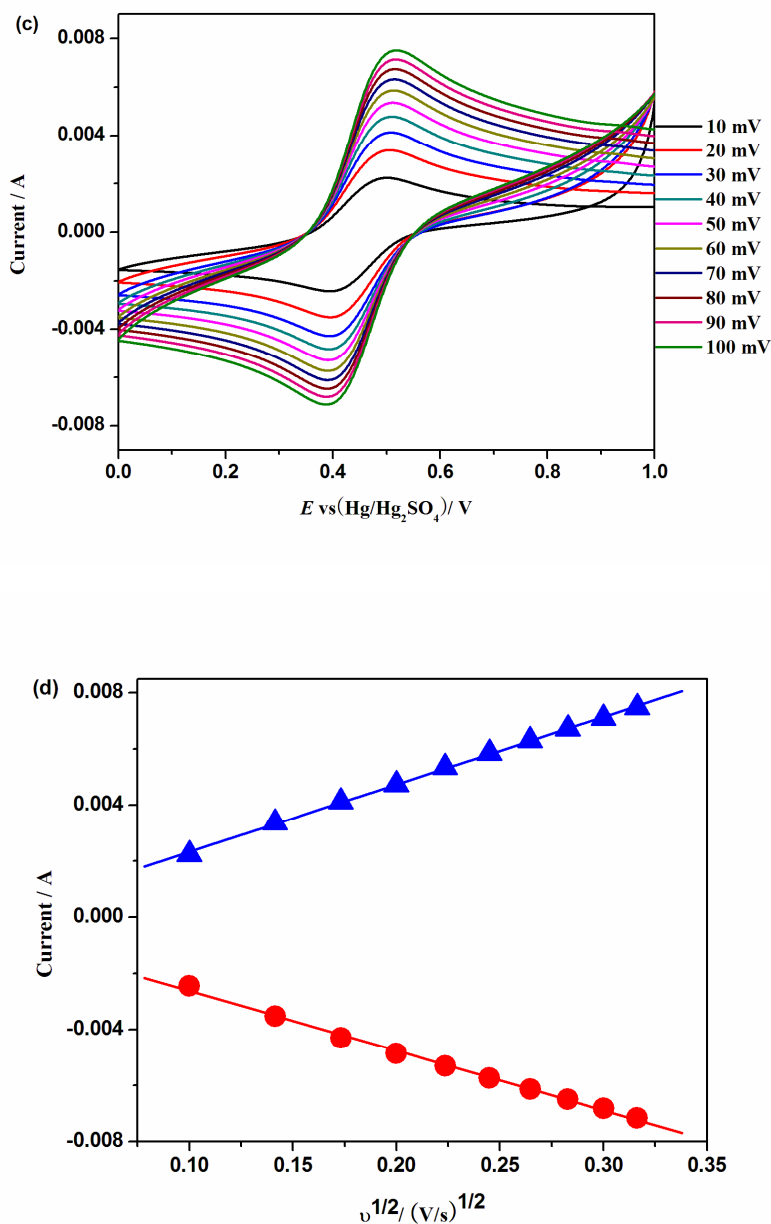
scan rate of 50 mV s^{-1}.

Fig. 5 (a) CV curves of the electrolyte (2.8 M V(V) / 5.0 M H_2SO_4) with 0.5 wt% CHPTAC on graphite electrode at room temperature at different scan rates and (b) corresponding relationship of oxidation and reduction current peak as a function of the square root of scan rate. (c) CV curves of the electrolyte (2.8 M V(V) / 5.0 M H_2SO_4) with 0.5 wt% MB on graphite electrode at room temperature at different scan

rates and (d) corresponding relationship of oxidation and reduction current peak as a
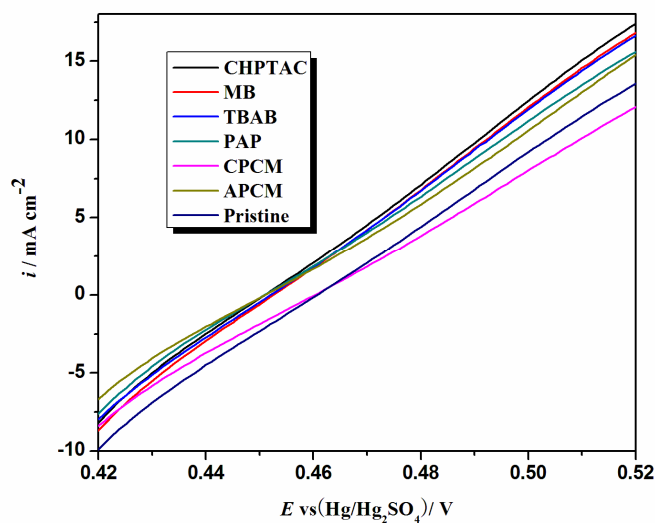
function of the square root of scan rate.

Fig. 6 Steady polarization curves for 2.8 M V(V) / 5.0 M H_2SO_4 solution with 0.5

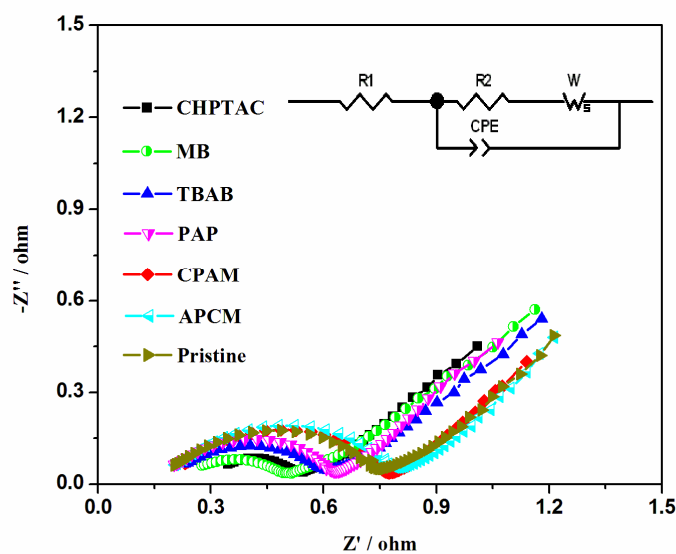wt% different acid additives on graphite electrode at a scan rate of 1 mV s^{-1}.

Fig. 7 Nyquist plots of the electrolytes with and without additives at room

temperature.

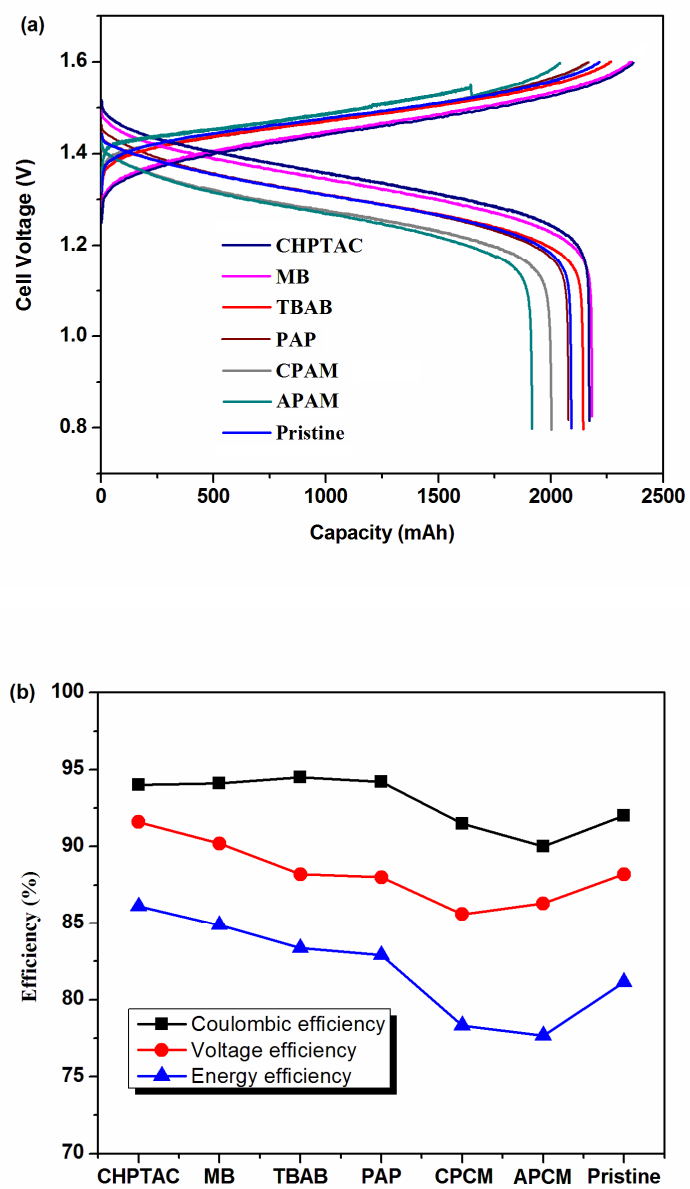**Fig. 8** (a) Charge-discharge curves and (b) different efficiency for VRB employed electrolyte with different ionic additives at current density of 20 mA cm^{-2} at room temperature.
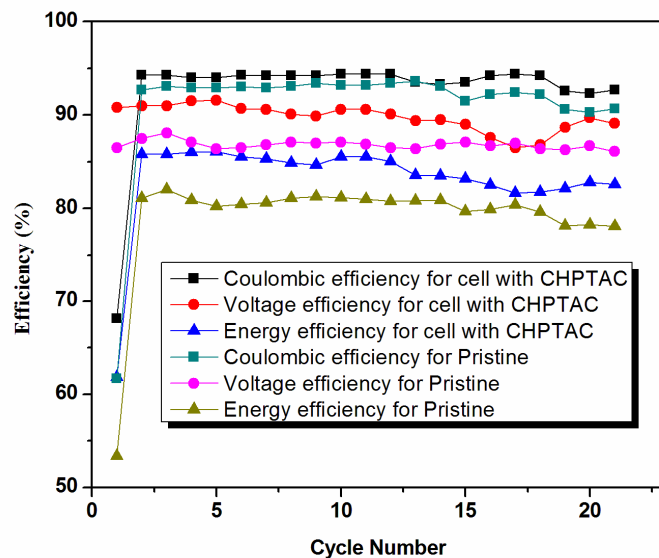
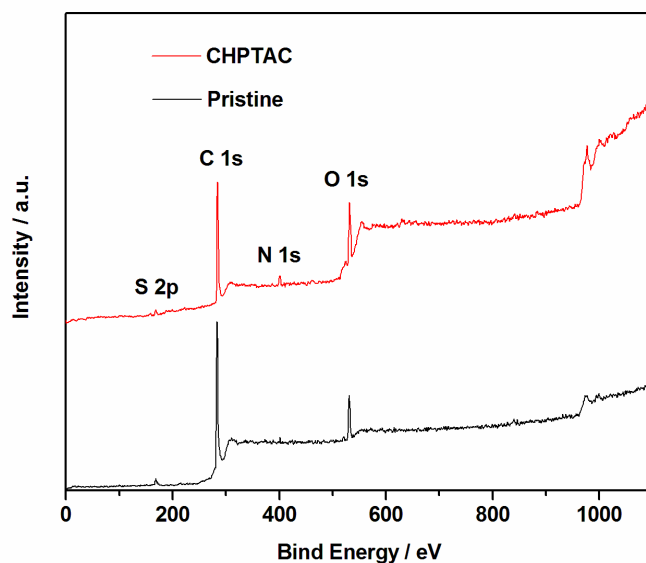**Fig. 9** Columbic, voltage and energy efficiency of VRB in cycling tests with and without 0.5 wt% CHPTAC.

Fig. 10 XPS spectra of graphite felt in the positive electrolyte with and without 0.5 wt% CHPTAC after cycling tests.

Table Captions

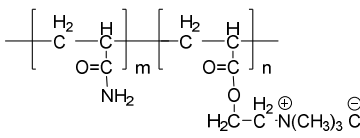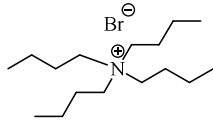**Table 1** Molecular structures of studied ionic organic additives.
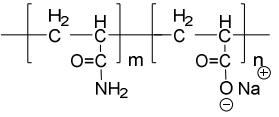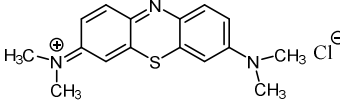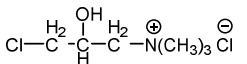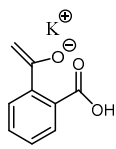
Chemical name (short form)	Molecular structure	Chemical name (short form)	Molecular structure
Cationic-type polyacrylamide (CPAM)		Tetrabutyl ammonium bromide (TBAB)	
Anionic-type polyacrylamide (APAM)		Methylene blue (MB)	
3-chloro-2hydroxyprop yl trimethyl ammonium chloride (CHPTAC)		Potassiumacidphthalate (PAP)	

Table 2 Effect of several additives on the thermal stability of 2.8 M V(V)/5 M H_2SO_4 electrolyte.

Additives (0.5 wt%)	Time to precipitation and concentration (M) of V(V) after 30 days (d) at different temperature (-5 °C, 10 °C and 30 °C)							
	-5 °C		10 °C		30 °C		45 °C	60 °C
CHPTAC	>30 d	2.6 M	>30 d	2.4 M	>30 d	2.2 M	4 d	3 h
MB	>30 d	2.3 M	>30 d	2.1 M	>30 d	1.9 M	>30 d	4 h
TBAB	>30 d	2.7 M	>30 d	2.5 M	26 d	2.3 M	2 d	2 h
PAP	>30 d	2.3 M	>30 d	2.2 M	23 d	2.0 M	35 h	2 h
CPAM	29 d	2.5 M	25 d	2.4 M	22 d	2.2 M	3 d	3 h
APAM	27 d	2.4 M	24 d	2.3 M	19 d	2.1 M	23 h	2 h
Pristine	24 d	2.4 M	19 d	2.1 M	12 d	2.0 M	18 h	1 h

Table 3 CV curves data of the electrolyte (2.8 M V(V) / 5.0 M H_2SO_4) with 0.5 wt%

ionic organic additives at different temperature on graphite electrode.

Temperature (°C)	Additives	CHPTAC	MB	TBAB	PAP	CPAM	APAM	Pristine
-5	ΔV_p (V)	0.17	0.15	0.18	0.20	0.24	0.23	0.20
	I_{pO}/I_{pR}	0.99	1.00	1.02	1.03	1.05	1.22	1.08
25	ΔV_p (V)	0.11	0.12	0.14	0.19	0.18	0.20	0.18
	I_{pO}/I_{pR}	1.03	1.03	1.04	1.03	1.09	0.92	1.09
45	ΔV_p (V)	0.10	0.10	0.11	0.17	0.16	0.16	0.15
	I_{pO}/I_{pR}	1.00	1.00	1.00	1.01	1.16	1.06	1.05

Table 4 Effect of ionic organic additives on the diffusion coefficient D_1 and D_2 of V(V)

species.

Additives (0.5 wt%)	Diffusion coefficient D_1 ($cm^2 s^{-1}$) and D_2 ($cm^2 s^{-1}$) of V(V) species with different additives at different temperature					
	-5 °C		25 °C		45 °C	
	D_1	D_2	D_1	D_2	D_1	D_2
CHPTAC	9.72×10^{-7}	7.89×10^{-7}	2.13×10^{-6}	1.73×10^{-6}	2.30×10^{-6}	1.87×10^{-6}
MB	6.55×10^{-7}	5.32×10^{-7}	1.88×10^{-6}	1.52×10^{-6}	2.03×10^{-6}	1.65×10^{-6}
TBAB	4.89×10^{-7}	3.97×10^{-7}	1.84×10^{-6}	1.49×10^{-6}	1.95×10^{-6}	1.58×10^{-6}
PAP	4.72×10^{-7}	3.83×10^{-7}	1.61×10^{-6}	1.31×10^{-6}	1.81×10^{-6}	1.47×10^{-6}
CPCM	3.64×10^{-7}	2.96×10^{-7}	1.45×10^{-6}	1.18×10^{-6}	1.56×10^{-6}	1.27×10^{-6}
APCM	3.54×10^{-7}	2.87×10^{-7}	1.34×10^{-6}	1.09×10^{-6}	1.42×10^{-6}	1.15×10^{-6}
Pristine	4.22×10^{-7}	3.61×10^{-7}	1.57×10^{-6}	1.27×10^{-6}	1.77×10^{-6}	1.44×10^{-6}

Table 5 Kinetic parameters by way of steady polarization for 2.8 M V(V) / 5.0 M H$_2$SO$_4$ solution with different ionic organic additives on graphite electrode at different temperature.

Additives (0.5 wt%)	Kinetic parameters for V(V) solution with different acid additives at different temperature								
	-5 °C			25 °C			45 °C		
	R_p (Ωcm^2)	i_0 (mAcm^{-2})	k_0 (10^{-5}cms^{-1})	R_p (Ωcm^2)	i_0 (mAcm^{-2})	k_0 (10^{-5}cms^{-1})	R_p (Ωcm^2)	i_0 (mAcm^{-2})	k_0 (10^{-5}cms^{-1})
CHPTAC	6.34	4.05	1.50	3.77	6.81	2.52	2.48	10.36	3.83
MB	6.49	3.96	1.47	3.82	6.72	2.49	2.58	9.96	3.69
TBAB	6.58	3.90	1.44	3.95	6.50	2.41	2.63	9.77	3.62
PAP	6.69	3.84	1.42	4.11	6.25	2.31	2.84	9.04	3.35
CPCM	6.85	3.75	1.39	4.29	5.99	2.22	2.96	8.68	3.21
APCM	7.07	3.63	1.34	4.78	5.37	1.99	3.15	8.15	3.02
Pristine	6.75	3.81	1.41	4.24	6.06	2.24	3.06	8.39	3.11

Table 6 Parameters resulting from fitting the impedance plots with the equivalent circuit model in Fig. 7.

Additives (0.5 wt %)	R_1/Ωcm^2	CPE/S sec^{-n} cm^{-2}		R_2/Ωcm^2	W, $Y_{0,2}$/S sec^{-5} cm^{-2}
		$Y_{0,1}$	n		
CHPTAC	0.2372	2.708×10^{-3}	1	0.1243	2.672
MB	0.2377	2.695×10^{-3}	0.9979	0.1830	2.597
TBAB	0.2515	2.544×10^{-3}	0.9896	0.2551	2.218
PAP	0.2546	2.411×10^{-3}	0.9865	0.3677	2.073
CPAM	0.2951	1.973×10^{-3}	0.9796	0.4298	1.676
APAM	0.2974	1.835×10^{-3}	0.9674	0.4639	1.568
Pristine	0.2748	2.196×10^{-3}	0.9465	0.3905	1.864

Table 7 The relative contents of the elements on the surface of graphite felt after cycling tests.

Element	Peak Binding Energy (eV)	CHPTAC (atom %)	Pristine (atom %)
S 2p	168.55	2.66	2.50
C 1s	284.25	58.94	76.42
N 1s	401.25	4.63	1.51
O 1s	531.90	33.77	19.57